





**Nonreciprocal coherent all-optical switching between magnetic multistates**T. Zalewski <sup>\*</sup>, V. A. Ozerov, A. Maziewski , I. Rzdolski , and A. Stupakiewicz <sup>†</sup>*Faculty of Physics, University of Białystok, 1L Ciołkowskiego, 15-245 Białystok, Poland*

(Received 30 July 2023; accepted 23 January 2024; published 22 February 2024)

We present experimental and computational findings of the laser-induced nonreciprocal motion of magnetization during ultrafast photomagnetic switching in garnets. We found distinct coherent magnetization precession trajectories and switching times between four magnetization states, depending on both directions of the light linear polarization and initial magnetic state. As a fingerprint of the topological symmetry, the choice of the switching trajectory is governed by an interplay of the photomagnetic torque and magnetic anisotropy. Our results open a plethora of possibilities for designing energy-efficient magnetization switching routes at arbitrary energy landscapes.

DOI: [10.1103/PhysRevB.109.L060303](https://doi.org/10.1103/PhysRevB.109.L060303)

**Introduction.** Understanding the interplay between topology, crystal symmetry, and the free energy landscape map is key for the manipulation of magnetic moments in complex systems. Control of spin dynamics at ultrashort timescales by various stimuli has recently become a vibrant research direction revolving around physical mechanisms acting on magnetization as well as their dynamical characteristics [1–4]. Steering the magnetization along energy-efficient routes across the magnetic anisotropy landscape requires the highly sought-after ability to control the torque. Multiple mechanisms have been suggested, including current modulation in spin-orbit torque systems [5,6], employing ultrashort acoustic pulses [7–9], and utilizing coherent phonon-magnon coupling [10–13]. In general, among the variety of methods, the ability to manipulate magnetization solely using laser pulses holds tremendous potential for future technologies, facilitating the fastest-ever data recording with minimal heat dissipation. On top of essentially thermal mechanisms of all-optical magnetization switching [14,15], of particular interest is the nonthermal photomagnetic excitation where spin-orbit interaction mediates the modification of the spin energy landscape through absorption of optical radiation. Over the last decades, a solid body of knowledge has been accumulated aiming at bringing the photomagnetism onto the ultrafast timescale and separating it from concomitant thermal and inverse magneto-optical effects [16–21]. Owing to its nonthermal nature, the dynamics of photomagnetism, in which magnetization is not quenched upon pulse laser irradiation, heavily relies on the magnetization precession. The latter is usually described by the Landau-Lifshitz-Gilbert (LLG) dynamics with a time-dependent effective magnetic field [22]. This highlights the importance of the topography of a magnetic landscape, which could play a key role in determining the magnetization switching conditions as well as the relevant dynamical characteristics. Materials with a cubic magnetic symmetry usually

have a large number of degenerate energy minima, and smaller angles between them facilitate the nonlinear regime of large-angle magnetization precession [23] and eventually all-optical switching [24].

Since the magnetization is set into motion through an ultrafast modification of the energy landscape, it is of utter importance to understand the optical response of the latter in detail. This dynamical topography can then be used advantageously, for example, reducing the energy consumption or accelerating the switching dynamics. The latter is particularly relevant in light of the recently demonstrated controllable magnetization reversal between two equilibrium states at the picosecond timescale [24]. The open questions that we address in this work pertain to the detailed analysis of the trajectories of the magnetization switching as well as the anatomy of the photomagnetic excitation in high-symmetry media. Employing a time-resolved magneto-optical imaging technique, we get valuable insights into the coherent dynamics of simultaneous switching of coexisting magnetic states by a single laser pulse. We demonstrate the existence of two nonequivalent switching trajectories in cubic photomagnetic yttrium-iron-garnet with Co ions (YIG:Co), whereas the forward and backward routes of magnetization can be chosen with the polarization of light. We further highlight the key role of an interplay between the torque and magnetic symmetries in the laser-induced motion of spins in coexisting magnetic domains. We argue that the apparent (almost twofold) difference in the switching times between the two pairs of states represents another fingerprint of the torque symmetry exhibiting coherent magnetization switching.

*Time-resolved multistate magnetization switching.* The photomagnetic YIG:Co(001) film is characterized by the predominantly cubic magnetic anisotropy with eight energy minima, with magnetization oriented close to the diagonals of the cubic unit cell [25,26] (see the Supplemental Material (SM) [27]). Among those minima, we focus on four [Fig. 1(a)] which exhibit the full richness of the magnetization dynamics upon photomagnetic excitation with a single

<sup>\*</sup>Corresponding author: [tmkzlwsk@uwb.edu.pl](mailto:tmkzlwsk@uwb.edu.pl)<sup>†</sup>Corresponding author: [and@uwb.edu.pl](mailto:and@uwb.edu.pl)

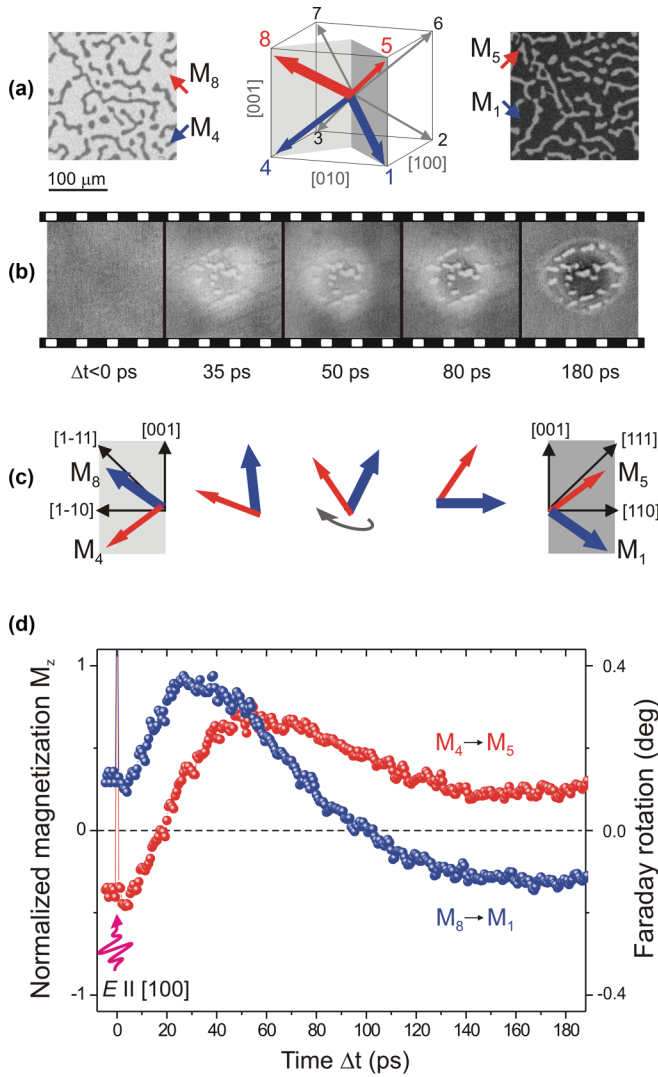


FIG. 1. Multistates magnetization switching in a cubic magnetic system. (a) Images of multistates magnetic domain structure and orientation of easy magnetization axes in YIG:Co films. (b) The differential stack of time-resolved images illustrating the transient dynamics of photomagnetic switching in YIG:Co. The experiment involved the use of a 50-fs single pump pulse with a fluence of  $50 \text{ mJ cm}^{-2}$  and polarization along  $E \parallel [100]$  direction in the garnet. (c) The sketch illustrates the motion and rotation of magnetization at domains for different delay time  $\Delta t$ . (d) The normalized out-of-plane component of magnetization  $M_z$  for the simultaneous switching between four magnetic states ( $M_8 - M_1$  and  $M_4 - M_5$ ).

50-fs pump laser pulse. To achieve the highest photomagnetic efficiency of the switching [28], the pump wavelength was set to 1300 nm (see [27]). In contrast to our previous observations [24], here we employed the highly sensitive time-resolved single-shot magneto-optical imaging technique [29] which allows for simultaneous observation of magnetization dynamics in coexisting magnetic phases and retrieve both the spatial and temporal dynamics of multidomain states. In particular, we monitored the laser-induced dynamics of the magnetization in domains depicted in Fig. 1(a) through transient variations of the Faraday rotation of the defocused probe beam at 650 nm wavelength.

To improve the signal-to-noise ratio, background images with the pump beam blocked were subtracted at each time delay, thus creating the presented stack of differential images of the normal [001] magnetization projection  $M_z$ . Selecting regions of interest within the borders of individual domains and integrating the variations over them, we obtained a set of traces corresponding to the laser-induced  $\Delta M_z$  dynamics in each of the magnetic states as a function of the optical delay between the pump and probe pulses  $\Delta t$  (see the SM [27]).

In the image sequence complemented by (or together with) a sketch of magnetization states in Figs. 1(b) and 1(c), we show that the magnetization switching occurs in both large ( $M_1$  and  $M_8$ ) and small ( $M_4$  and  $M_5$ ) domains simultaneously. We note that the pattern of the small domains remains constant during the entire experiment, thus confirming the nonthermal nature of the photomagnetic switching. Interestingly, after about 30 ps the magnetization starting its dynamics from the  $M_1$  direction obtains the transient perpendicular state to the sample plane. This is in contrast with the previously reported [24] magnetization switching between the canted states in YIG:Co via the in-plane direction.

A typical example of the experimental  $\Delta M_z(\Delta t)$  traces in the two states with opposite normal magnetization components is shown in Fig. 1(d), illustrating the switching along the  $M_8 \rightarrow M_1$  and  $M_4 \rightarrow M_5$  routes with the  $E \parallel [100]$  pump pulses. It is seen that the trajectories are clearly asymmetric. The sketch in Fig. 1(c) illustrates the rotation of the magnetization pair in adjacent domains (red and blue arrows), where the transient variations of the angle between them are inextricably linked to the inequality of the two trajectories.

Similar measurements performed when all eight different magnetic states were prepared and illuminated with light at one of the two orthogonal polarizations ( $E \parallel [100]$  and  $E \parallel [010]$  directions) revealed that only two unique time traces of  $\Delta M_z(\Delta t)$  can be observed (see the SM [27]). Thus, all switching trajectories can be assigned to either type I or type II, depending on the initial magnetization state and pump polarization. In Fig. 2(a) we show the averaged traces of both types for the orthogonal pump polarizations along the [100] and [010] directions, and the inequivalence of these trajectories becomes glaringly apparent. This observation is highly surprising in light of the fourfold crystalline symmetry and magnetic anisotropy of the garnet. To understand the physical origins of the dissimilarity of the two trajectories, we decomposed them into even and odd contributions. These are shown in Fig. 2(b) with green and black full data points, respectively. Notably, the even part closely resembles the average over multiple domains, a steplike switching trace reported previously [24]. It is seen that by 100 ps, the switching is already completed, and the remaining minute variations are related to the relaxation of magnetization within the corresponding potential minimum. On the other hand, the odd part exhibits a strongly damped oscillatory character, highlighting the precessional character of the switching dynamics in general. It is the odd contribution that is responsible for the nonreciprocal switching seen in Fig. 2(a): the switching along the  $M_4 \rightarrow M_5$  route and back proceeds along the different trajectories.

We argue that the odd, nonreciprocal contribution can be understood as a fingerprint of the interplay between the torque symmetry and the coherent magnetization dynamics.

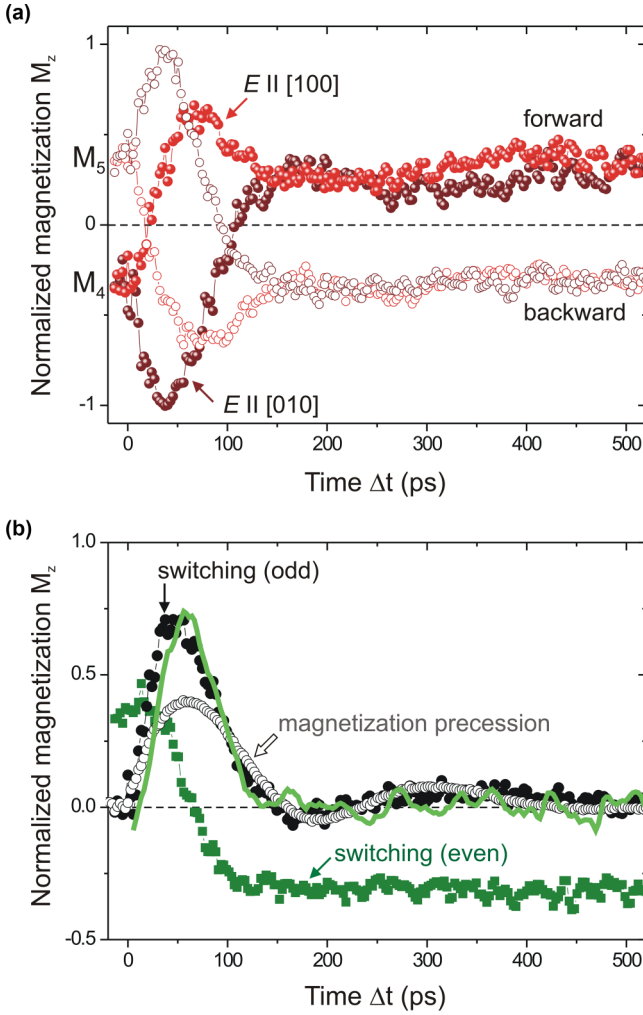


FIG. 2. Nonreciprocal of all-optical magnetization switching. (a) Pump polarization effect on magnetization trajectory enabling selecting switching trajectory and final state for orthogonal orientation of laser pump polarization along [100] and [010] directions in YIG:Co film. (b) The differential signal of switched states (close black points) compared to the measured magnetization precession (open points) below the threshold level of switching. The even and odd contribution of photomagnetic switching. The green solid line is the scaled derivative of the even component of photomagnetic switching.

The solid line in Fig. 2(b) shows the (scaled) time derivative of the even contribution. Its striking reminiscence of the odd part suggests that the latter originates in the precession of magnetization when moving along the switching route. This results in the emergence of the orthogonal component  $dM/dt$  since  $(M dM/dt) = 0$ . The sign of this orthogonal component is governed by the direction of movement along the switching route, thus giving rise to the odd contribution to the magnetization dynamics. In other words, a new curvilinear reference frame can be introduced where the even contribution depicting the genuine switching route is bereft of any rotational part. In such a reference frame, the LLG equation will be transformed accordingly, acquiring an additional term similarly to the mechanical equations of motion in a rotating reference frame. This additional term can be viewed as a fictitious magnetic field giving rise to the magnetization dynamics in the direction

orthogonal to the switching route, or the aforementioned odd contribution. The characteristic shape of the normal projection of this contribution is then determined by the change rate of  $M_z$  along the switching route, in agreement with Fig. 2(b).

*Photomagnetic torque symmetry.* To get further insight into the laser-induced asymmetry of the magnetization switching trajectories, we performed a tensor analysis of the photomagnetic excitation along the lines discussed in [24]. In particular, the photomagnetic Hamiltonian contribution reads

$$\mathcal{H}_{p-m} = \hat{\beta} \mathbf{E} \mathbf{E}^* \mathbf{M} \mathbf{M}, \quad (1)$$

where  $E$  is the electric field of the optical pump and  $\hat{\beta}$  is a fourth-order polar tensor responsible for the photomagnetic susceptibility [28]. In the reference frame aligned with the main crystal axes, the initial (equilibrium) magnetization  $M$  has all three nonzero components ( $M_x, M_y, M_z$ ). Our analysis shows that the asymmetry of the trajectories is inextricably linked to the cubic symmetry of the photomagnetic medium. In particular, we consider a cubic garnet crystal with an  $m3m$  point group symmetry. Assuming normal pump incidence so that  $E_x \parallel [100]$ ,  $E_y \parallel [010]$ ,  $E_z = 0$ , only three nonzero  $\hat{\beta}$  components remain relevant in our case (see the SM [27]). The photomagnetic excitation of spin dynamics is mediated by the effective photomagnetic field  $\mathbf{H}_L = -\frac{\partial \mathcal{H}}{\partial \mathbf{M}}$ . It then exerts a torque  $T$  on magnetization, thus setting it into motion according to the LLG formalism  $\frac{\partial \mathbf{M}}{\partial t} = -\mathbf{M} \times \mathbf{H}_L$ . Directly after the optical excitation, the out-of-plane laser-induced magnetization dynamics takes the following form:

$$\frac{\partial M_z}{\partial t} = \beta' (E_x^2 - E_y^2) M_x M_y + 2\beta'' E_x E_y (M_x^2 - M_y^2), \quad (2)$$

Here  $\beta'$  and  $\beta''$  are the linear combinations of the nonzero  $\beta$  components:  $\beta' \equiv (\beta_3 - \beta_1)$ ,  $\beta'' \equiv 2\beta_2$  (see the SM [27]). Two main conclusions can be drawn from this result. First, consider the two initial magnetic states  $M_8$  and  $M_4$ , as indicated in Fig. 1, that is, with identical in-plane magnetization components but opposite out-of-plane ones,  $M_z^8 = -M_z^4$ . Without the loss of generality, we refer to them as the “up” and “down” states, although the choice of up and down directions is arbitrary. Then, since it is even with respect to  $M_z$ , the normal component of the magnetization dynamics  $\frac{\partial M_z}{\partial t}|_0$  will be the same for these two states. In other words, the up state will get the momentum towards the final down state of the switching process, whereas the down state will start its motion in the direction away from its destination. It is thus seen that the asymmetry of the switching trajectories is introduced immediately after the photomagnetic excitation, and is governed by the tensor nature of the photomagnetic effect and the cubic crystal symmetry.

Second, consider an excitation with linearly polarized light. Because the uniaxial anisotropy in our garnet film is much weaker than the cubic one, the equilibrium magnetization directions are close to the diagonals of the cubic unit cell. We thus can assume  $M_x \approx M_y$  so that the first term in the normal torque component dominates. As such, the in-plane symmetry of the excitation is given by the  $E_x^2 - E_y^2$  term, reducing to  $E^2 \cos 2\varphi$ , where  $\varphi$  indicates the light polarization. Effectively, the in-plane symmetry of the photomagnetic switching is lowered from *fourfold* to *twofold*, which can be illustrated by rotating the polarization of the incident

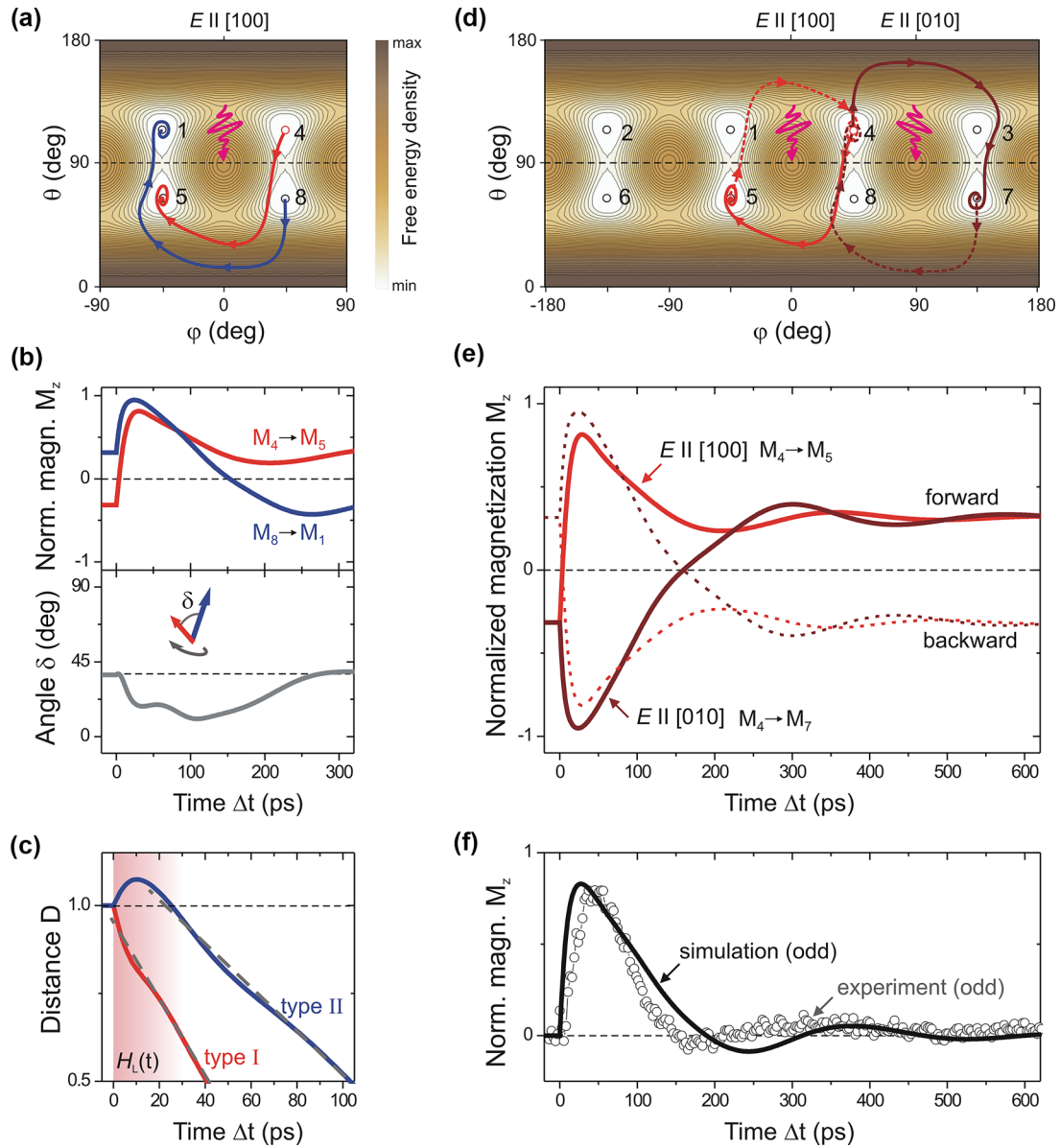


FIG. 3. Trajectories of magnetization dynamics on a fourfold-symmetric energy landscape. (a) The simulated energy map with multi-states switching for different initial states (b) The trajectories of a normalized out-of-plane component  $M_z$  with variations of the angle between moving vectors. (c) The evolution of the distance to destination  $D$  highlighting type I and type II trajectories (dashed grey lines are the linear fitting). The red-shaded area shows the photoinduced anisotropy field  $H_L(t)$  with a lifetime of about 20 ps. (d) The full simulated energy map showing different magnetization trajectories induced by the  $E \parallel [100]$  or  $E \parallel [010]$  light pulses. (e) Nonreciprocity of the all-optical switching caused by the change in the light pulse polarization plane (forward and backward switching). (f) Differential (odd) contribution to  $E \parallel [100]$  and  $E \parallel [010]$  trajectories responsible for the nonreciprocity compared with the experimental data.

light from the  $[100]$  to the  $[010]$  direction. This leads to the reversal of the switching asymmetry: the normal component of the torque changes its sign, and thus the switching trajectories of the two considered initial magnetic states will be flipped. All these implications are in striking agreement with the experimental findings.

*Modeling the trajectories of photomagnetic switching.* Employing the extended LLG model of photomagnetic switching [28] in which laser pulses act as a perturbation to the free energy density, we simulated the trajectories for the multi-states magnetization switching in a real YIG:Co(001) thin

film. In the simulations, a tetragonal distortion of the cubic magnetic symmetry has been introduced (see the SM [27]). In Fig. 3(a), the trajectories of magnetization switching induced by a normally incident laser pulse with the electric field  $E$  are shown on the map, highlighting the polarization selectivity. The variations of the  $M_z$  observed experimentally are summarized in Fig. 3(b). Notably, the difference in the movement rates of the two simultaneously precessing magnetization vectors is enabled by the lack of coupling between them. This is further confirmed in the simulations where the angle between the two magnetization vectors (bottom panel) exhibits strong

variations during their switching. Because magnetodipole interaction in adjacent domains is too weak and manifests on the nanosecond timescale at best, the two magnetization vectors move independently.

It is apparent that the model captures the pronounced asymmetry of the switching trajectories, thus paving the way for further analysis. In particular, we turn to the apparent dissimilarity of the characteristic timescales when the magnetization takes either one of the two available switching routes. To quantify this, we calculated the evolution of the normalized distance to the route destination as

$$D = \sqrt{\sum_i (M_i(t) - M_i^f)^2} / D_0, \quad (3)$$

where  $M_i^f$  are the magnetization components of the final point on the trajectory and  $D_0$  is the initial distance to the destination. A striking almost twofold difference in the movement rates along the two trajectories [Fig. 3(c)] corroborates their inequivalence and enables the qualitative distinction between the faster and slower (type I and type II as above) switching routes.

Last, the simulations reproduce the nonequivalence of the two types of trajectories in terms of transient variations of the normal magnetization component  $\Delta M_z(\Delta t)$  [Fig. 3(e)]. Depending on the polarization (parallel to either [100] or [010]) of the optical pump pulse, magnetization selects the fast or slow trajectory towards its destination, in agreement with the experimentally found nonreciprocity [cf. Fig. 2(a)]. Similarly, the simulated odd component in Fig. 3(f) exhibits an oscillating character, again correlating well with the experimental observations and reinforcing our understanding of its origin in the sign of the initially produced photomagnetic torque.

*Discussion.* The apparent non-reciprocity of the photomagnetic switching routes is enabled by two main factors. First, it is only possible when the switching is precessional in nature, as opposed to the thermal mechanisms accompanied by the magnetization quenching. Second, it requires an intricate interplay of the excitation tensor symmetry and magnetic energy landscape. In particular, in a uniaxial magnetic system, the observed asymmetry is impossible, which makes it difficult to imagine the discussed nonreciprocity in amorphous alloys where the dominant uniaxial contribution

of magnetic anisotropy is often governed by the growth direction. Cubic magnetic crystals thus represent an attractive class of materials for exploring the richness of the nonthermal excitation of nonreciprocal magnetization dynamics. They constitute a promising playground for engineering magnetic energy landscapes in order to achieve faster and more efficient unidirectional switching. In particular, the change in cubic and uniaxial growth-induced anisotropy enables encoding materials with a spatial distribution of states with different energy thresholds, which can dramatically reduce the switching energy.

The approach developed in our work can be extended towards more sophisticated systems featuring additional external stimuli and physically rich interaction mechanisms. In particular, thermal demagnetization can be accounted for on equal footing by introducing Landau-Lifshitz-Bloch formalism. Moreover, there is tremendous potential in utilizing strain (either dc or phonon-induced) or auxiliary magnetic and electric fields to control the effective field of the anisotropy. Taking advantage of the extremely large phase space with these fields as control parameters, the switching between multiple domain states holds promise for the advancement of multilevel magnetic memories. In particular, the inequality of the switching trajectories indicates the possibility of simultaneously steering a set of magnetizations from one combination of states to another with a single stimulus, realizing a multidimensional magnetization switching. By encoding information not only in binary but in a set of magnetization states (e.g., logical combinations of 00, 01, 10, 11, etc.), a greater number of distinct levels can be achieved, allowing for higher data storage density.

*Acknowledgments.* We acknowledge support from Foundation for Polish Science Grant No. POIR.04.04.00-00-413C/17-00 and the European Union's Horizon 2020 Research and Innovation Programme under Marie Skłodowska-Curie Grant Agreement No. 861300 (COMRAD). We thank Prof. A. Zvezdin for the fruitful discussions.

A.S. conceived the project with contributions from I.R. The measurements were performed by T.Z. The simulations were performed by V.A.O., and T.Z. I.R. performed the symmetry analysis. A.S. and I.R. co-wrote the manuscript with contributions from T.Z. and A.M. The project was coordinated by A.S.

The authors declare no competing interests.

- 
- [1] A. Kirilyuk, A. V. Kimel, and T. Rasing, Ultrafast optical manipulation of magnetic order, *Rev. Mod. Phys.* **82**, 2731 (2010).
- [2] E. Y. Vedmedenko, R. K. Kawakami, D. D. Sheka, P. Gambardella, A. Kirilyuk, A. Hirohata, C. Binek, O. Chubykalo-Fesenko, S. Sanvito, B. J. Kirby *et al.*, The 2020 magnetism roadmap, *J. Phys. D: Appl. Phys.* **53**, 453001 (2020).
- [3] A. V. Kimel and M. Li, Writing magnetic memory with ultrashort light pulses, *Nat. Rev. Mater.* **4**, 189 (2019).
- [4] T. Kubacka, J. A. Johnson, M. C. Hoffmann, C. Vicario, S. De Jong, P. Beaud, S. Grübel, S. W. Huang, L. Huber, L. Patthey *et al.*, Large-Amplitude spin dynamics driven by a THz pulse in resonance with an electromagnon, *Science* **343**, 1333 (2014).
- [5] A. Brataas, A. D. Kent, and H. Ohno, Current-Induced torques in magnetic materials, *Nat. Mater.* **11**, 372 (2012).
- [6] S. Manipatruni, D. E. Nikonov, C. C. Lin, T. A. Gosavi, H. Liu, B. Prasad, Y. L. Huang, E. Bonturim, R. Ramesh, and I. A. Young, Scalable energy-efficient magnetoelectric spin-orbit logic, *Nature (London)* **565**, 35 (2019).
- [7] A. V. Scherbakov, A. S. Salasyuk, A. V. Akimov, X. Liu, M. Bombeck, C. Brüggemann, D. R. Yakovlev, V. F. Sapega, J. K. Furdyna, and M. Bayer, Coherent magnetization precession

- in ferromagnetic (Ga,Mn)As induced by picosecond acoustic pulses, *Phys. Rev. Lett.* **105**, 117204 (2010).
- [8] O. Kovalenko, T. Pezeril, and V. V. Temnov, New concept for magnetization switching by ultrafast acoustic pulses, *Phys. Rev. Lett.* **110**, 266602 (2013).
- [9] V. S. Vlasov, A. M. Lomonosov, A. V. Golov, L. N. Kotov, V. Besse, A. Alekhin, D. A. Kuzmin, I. V. Bychkov, and V. V. Temnov, Magnetization switching in bistable nanomagnets by picosecond pulses of surface acoustic waves, *Phys. Rev. B* **101**, 024425 (2020).
- [10] D. Afanasiev, I. Razdolski, K. M. Skibinsky, D. Bolotin, S. V. Yagupov, M. B. Strugatsky, A. Kirilyuk, T. Rasing, and A. V. Kimel, Laser excitation of lattice-driven anharmonic magnetization dynamics in dielectric FeBO<sub>3</sub>, *Phys. Rev. Lett.* **112**, 147403 (2014).
- [11] S. F. Maehrlein, I. Radu, P. Maldonado, A. Paarmann, M. Gensch, A. M. Kalashnikova, R. V. Pisarev, M. Wolf, P. M. Oppeneer, J. Barker *et al.*, Dissecting spin-phonon equilibration in ferrimagnetic insulators by ultrafast lattice excitation, *Sci. Adv.* **4**, eaar5164 (2018).
- [12] A. Stupakiewicz, C. S. Davies, K. Szerenos, D. Afanasiev, K. S. Rabinovich, A. V. Boris, A. Caviglia, A. V. Kimel, and A. Kirilyuk, Ultrafast phononic switching of magnetization, *Nat. Phys.* **17**, 489 (2021).
- [13] A. S. Disa, M. Fechner, T. F. Nova, B. Liu, M. Först, D. Prabhakaran, P. G. Radaelli, and A. Cavalleri, Polarizing an antiferromagnet by optical engineering of the crystal field, *Nat. Phys.* **16**, 937 (2020).
- [14] I. Radu, K. Vahaplar, C. Stamm, T. Kachel, N. Pontius, H. A. Dürr, T. A. Ostler, J. Barker, R. F. L. Evans, R. W. Chantrell *et al.*, Transient ferromagnetic-like state mediating ultrafast reversal of antiferromagnetically coupled spins, *Nature (London)* **472**, 205 (2011).
- [15] T. A. Ostler, J. Barker, R. F. L. Evans, R. W. Chantrell, U. Atxitia, O. Chubykalo-Fesenko, S. El Moussaoui, L. Le Guyader, E. Mengotti, L. J. Heyderman *et al.*, Ultrafast heating as a sufficient stimulus for magnetization reversal in a ferrimagnet, *Nat. Commun.* **3**, 666 (2012).
- [16] A. Chizhik, I. Davidenko, A. Maziewski, and A. Stupakiewicz, High-Temperature photomagnetism in Co-Doped yttrium iron garnet films, *Phys. Rev. B* **57**, 14366 (1998).
- [17] F. Hansteen, A. Kimel, A. Kirilyuk, and T. Rasing, Femtosecond photomagnetic switching of spins in ferrimagnetic garnet films, *Phys. Rev. Lett.* **95**, 047402 (2005).
- [18] A. M. Kalashnikova, A. V. Kimel, R. V. Pisarev, V. N. Gridnev, A. Kirilyuk, and T. Rasing, Impulsive generation of coherent magnons by linearly polarized light in the easy-plane antiferromagnet FeBO<sub>3</sub>, *Phys. Rev. Lett.* **99**, 167205 (2007).
- [19] F. Atoneche, A. M. Kalashnikova, A. V. Kimel, A. Stupakiewicz, A. Maziewski, A. Kirilyuk, and T. Rasing, Large ultrafast photoinduced magnetic anisotropy in a cobalt-substituted yttrium iron garnet, *Phys. Rev. B* **81**, 214440 (2010).
- [20] I. Yoshimine, T. Satoh, R. Iida, A. Stupakiewicz, A. Maziewski, and T. Shimura, Phase-Controllable spin wave generation in iron garnet by linearly polarized light pulses, *J. Appl. Phys.* **116**, 043907 (2014).
- [21] L. A. Shelukhin, V. V. Pavlov, P. A. Usachev, P. Y. Shamray, R. V. Pisarev, and A. M. Kalashnikova, Ultrafast laser-induced changes of the magnetic anisotropy in a low-symmetry iron garnet film, *Phys. Rev. B* **97**, 014422 (2018).
- [22] J. Stohr and H. C. Siegmann, *Magnetism*, 1st ed. (Springer, Berlin, 2006).
- [23] A. Frej, I. Razdolski, A. Maziewski, and A. Stupakiewicz, Nonlinear subswitching regime of magnetization dynamics in photomagnetic garnets, *Phys. Rev. B* **107**, 134405 (2023).
- [24] A. Stupakiewicz, K. Szerenos, D. Afanasiev, A. Kirilyuk, and A. V. Kimel, Ultrafast nonthermal photo-magnetic recording in a transparent medium, *Nature (London)* **542**, 71 (2017).
- [25] P. Görnert, M. Nevřiva, J. Šimšová, W. Andrä, W. Schüppel, P. Šumšál, and R. Bubáková, Co containing garnet films with low magnetization, *Phys. Status Solidi* **74**, 107 (1982).
- [26] A. Maziewski, Unexpected magnetization processes in YIG + Co films, *J. Magn. Magn. Mater.* **88**, 325 (1990).
- [27] See Supplemental Material at <http://link.aps.org/supplemental/10.1103/PhysRevB.109.L060303> for details on the methods used, including information on the material, experimental technique, photomagnetic symmetry analysis, and numerical simulation of magnetization trajectories. It also includes Refs. [29–32].
- [28] A. Stupakiewicz, K. Szerenos, M. D. Davydova, K. A. Zvezdin, A. K. Zvezdin, A. Kirilyuk, and A. V. Kimel, Selection rules for all-optical magnetic recording in iron garnet, *Nat. Commun.* **10**, 612 (2019).
- [29] T. Zalewski and A. Stupakiewicz, Single-Shot imaging of ultrafast all-optical magnetization dynamics with a spatiotemporal resolution, *Rev. Sci. Instrum.* **92**, 103004 (2021).
- [30] A. Maziewski, K. Mroczek, A. Stankiewicz, M. Tekielak, and M. Kisielewski, Advance in Magneto-Optics, in *Proceedings of the 2nd International Symposium in Magneto-Optics*, Fiz. Nizk. Temp. 18, Suppl. No. S1 (1992), pp. 377–381.
- [31] Y. Hashimoto, A. R. Khorsand, M. Savoini, B. Koene, D. Bossini, A. Tsukamoto, A. Itoh, Y. Ohtsuka, K. Aoshima, A. V. Kimel *et al.*, Ultrafast time-resolved magneto-optical imaging of all-optical switching in GdFeCo with femtosecond time-resolution and a Mm spatial-resolution, *Rev. Sci. Instrum.* **85**, 063702 (2014).
- [32] F. Steinbach, N. Stetzuhn, D. Engel, U. Atxitia, C. Von Korff Schmising, and S. Eisebitt, Accelerating double pulse all-optical write/erase cycles in metallic ferrimagnets, *Appl. Phys. Lett.* **120**, 112406 (2022).